ADVANCED MATERIALS

DOI: 10.1002/adma.200801579

Supercritical Continuous-Microflow Synthesis of Narrow Size Distribution Quantum Dots**

By *Samuel Marre, Jongnam Park, Jane Rempel, Juan Guan, Moungi G. Bawendi,** and *Klavs F. Jensen**

Colloidal semiconductor quantum dots (QDs) have been used in biological imaging,[1] electroluminescent devices,[2] and lasers[3] due to their size-tunable optical properties and chemical stability. Most of these applications require highly crystalline samples with narrow size distributions, which are often difficult to achieve in a single-step batch process with its often poor control of reaction conditions. Synthesis of QDs in microfluidic devices offers several advantages over conventional macroscale chemical processes,[4] including enhancement of mass and heat transfer,[5] reproducibility,[6] potential for sensor integration for in situ reaction monitoring,[7] rapid screening of parameters, and low reagent consumption during optimization.[8] Previous studies have realized the continuous synthesis of CdSe QDs at atmospheric pressure using single-phase laminar flow microreactor designs.[6,9] One difficulty of these synthetic procedures is the requirement for solvents that can both dissolve the precursors at ambient conditions and also remain liquid over the entire operating-temperature range (25 °C to 350 °C), significantly limiting the set of solvents, ligands, and precursors that are compatible with continuous flow systems. Furthermore, the solvents that are available are typically very viscous ($500\,\mu Pa \cdot s < \eta < 1500\,\mu Pa \cdot s$), leading to slow mixing, broad residence-time distributions (RTD), and as a consequence, broad QD-size distributions (typically >10%). Segmentation of the reacting phase with an immiscible phase[10] can overcome such limitations by narrowing the RTD and improving reactant mixing.[11,12] Application of segmented flow for continuous synthesis of narrowly distributed CdSe QDs has been previously demonstrated for liquid–gas,[13] and liquid–liquid[14] segmented flows. However, even with flow segmentation, limitations on the number of compatible chemistries and the limited number of available high-boiling-point solvents have been major obstacles in the rapid adoption of microreactors as universal platforms for QD synthesis.

One way of improving syntheses in microreactors is to perform experiments at high pressure. Indeed, at sufficiently high pressure, virtually any common solvent, precursor, and ligand will either remain liquid or become supercritical (sc) at the temperatures required for QD synthesis. In the supercritical regime, properties of the fluid can be tuned from liquid-like to gas-like,[15] displaying the high miscibility and fast diffusion rates typical of gasses, but with sufficiently high densities for solubilizing a wide range of compounds of low to medium polarity, typical of liquids. The supercritical-fluid technology has been successfully applied to materials processing as an alternative to conventional solvents to achieve the synthesis of both organic[16] and inorganic[17] materials. In microreactors, the low viscosities of supercritical fluids can be used to overcome the inherent limitations of conventional liquid solvents, leading to faster mixing and narrower residence-time distributions. These advantages were recently highlighted in catalytic hydrogenation reactions and esterification in supercritical CO_2.[18,19] Using macroscale batch reactors, QDs have been synthesized in supercritical fluids,[20] but in a noncontinuous-operation mode.

In this communication, we demonstrate the continuous microflow synthesis of CdSe QDs at high pressure both in a conventional high-boiling-point solvent, squalane, and also in liquid or supercritical hexane (sc-hexane). We explore the influence of several key parameters, including the phase of the solvent, the initial concentration of precursors, the temperature, and the residence time on the QD size, size distribution, and the concentration of nuclei. We show that synthesis at supercritical conditions significantly narrows the size distribution of CdSe QDs.

All experiments were performed in Silicon/Pyrex microreactors that allow for easy optical access and sustain high pressures.[21] The schematic of the experimental set-up is shown in Figure 1. The microreactor consisted of a 400 μm wide and 250 μm deep channel with a 0.1 m long mixing zone maintained at room temperature and a 1 m long reaction zone heated up to 350 °C. The two zones were separated by a thermally isolating halo etch that allowed for a temperature gradient of over 25 °C mm^{-1}. The entire set-up was first pressurized from the inlet to the outlet using a nitrogen gas cylinder. Thereafter, the nitrogen valve was closed and the two precursor solutions were delivered independently using a high-pressure syringe pump, insuring good control of the flow rate.

[*] Prof. M. G. Bawendi, Dr. J. Park, J. Guan
Department of Chemistry, Massachusetts Institute of Technology
77 Massachusetts Avenue, 6-221, MA02139 (USA)
E-mail: mgb@mit.edu
Prof. K. F. Jensen, Dr. S. Marre, Dr. J. Rempel
Department of Chemical Engineering
Massachusetts Institute of Technology
77 Massachusetts Avenue, 66-342, MA02139 (USA)
E-mail: kfjensen@mit.edu

[**] S. M. and J. P. have contributed equally to this work. This research was funded in part by the NSF (DMR 02-13282, CHE 0714189) and the US Army Research Office through the Institute for Soldier Nanotechnology. J. Park was supported by the Korean research Foundation Grant funded by the Korean Government (KRF-2006-214-D00038).

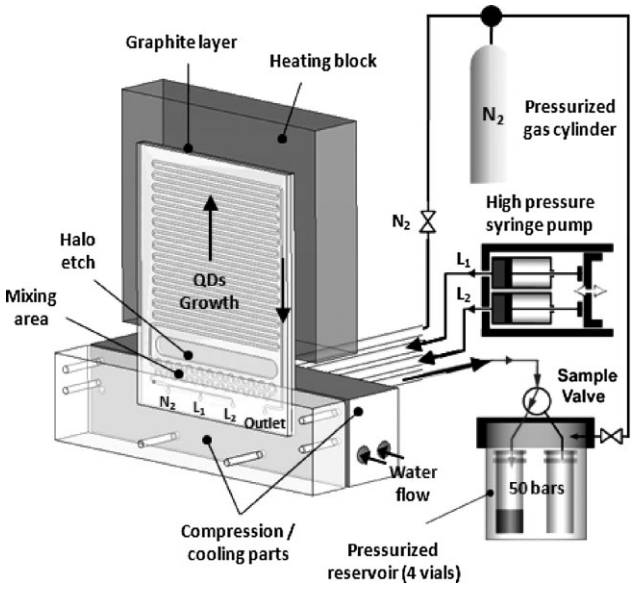

Figure 1. Experimental set-up including a high-pressure high-temperature microreactor, a compression-cooling aluminum part, a high-pressure syringe pump, a 5-way high-pressure valve, and a high-pressure reservoir containing 4 vials.

The precursor solutions were then mixed at room temperature prior to entering the high-temperature reaction zone, where the nucleation and growth of QDs occurred. The fluid exited the reactor in the low temperature zone, quenching QD growth. A high-pressure reservoir containing four vials was used to recover the samples without depressurizing the system, using a 5-way high-pressure valve.

Synthesis of CdSe QDs was carried out at 5 MPa. While maintaining a precursor ratio Cd:Se of 1, we varied the concentration of Cd between 3.8×10^{-3} M and 7.6×10^{-2} M. The residence time (t_R) was tuned from 30 to 150 s by varying the flow rate. To separate the supercritical effect from that of the solvent, experiments were performed at 210 °C, corresponding to the liquid phase for both hexane and squalane, and at 270 °C, corresponding to the supercritical phase for hexane ($T_c = 234.7$ °C and $p_c = 3.03$ MPa).[22] Physical characteristics of the two solvents at the experimental conditions are summarized in Table 1.[23]

Typical photoluminescence (PL) spectra as a function of residence time for CdSe QDs synthesized in liquid squalane and sc-hexane at 270 °C and 5 MPa with a precursor concentration of 3.8×10^{-3} M, as well as the corresponding QD-size distributions (d_{CdSe}) obtained from transmission electron microscopy (TEM) measurements, are shown in Figure 2. The optical absorption (not shown) and emission spectra (Fig. 2) were used to estimate the mean size, size distribution, and concentration of nuclei (Fig. 3). The average QD diameter (d_{avg}) was determined using the wavelength at the emission maximum.[24] The concentration of the nuclei in the growth solution was obtained based on the optical density and absorbance cross-section at 350 nm.[25] The size distribution percentage (σ_d/d_{avg}) was calculated from the PL peak width, assuming a single QD-emission linewidth of 50 meV. Although the choice of this value changes the estimated size distribution somewhat, the resulting trends remain the same.

For synthesis in both squalane and sc-hexane, the size of the QDs increases with residence time (Fig. 3a), leading to a red shift in the PL spectra (Fig. 2). Figure 3b shows that the total number of nuclei remains approximately constant, suggesting that in the range of residence times considered we observe only QD growth, in the absence of concurrent nucleation. Finally, as the QD size increases with an increase in the residence time, the width of the size distribution decreases (Fig. 3c). Variation in the precursor concentration does not alter these trends; however, increasing the concentration of precursors leads to an increase in both the concentration of nuclei and the mean QD size, as well as a slight increase in the size distribution.

Indeed, for higher concentrations more nuclei are formed, due to an increase in the supersaturation. In addition, more precursors remain in the solution after the nucleation step, allowing further growth and formation of larger QDs. The

Table 1. Phase, density, and viscosity of hexane and squalane as a function of temperature at $P = 5$ MPa.

T	Hexane			Squalane		
(°C)	Phase	Density (g mL^{-1})	η (μPa · s)	Phase	Density (g mL^{-1})	η (μPa s)
270	SC	0.27	33.5	Liquid	0.66	619.6
210	Liquid	0.45	74.7	Liquid	0.70	927.3

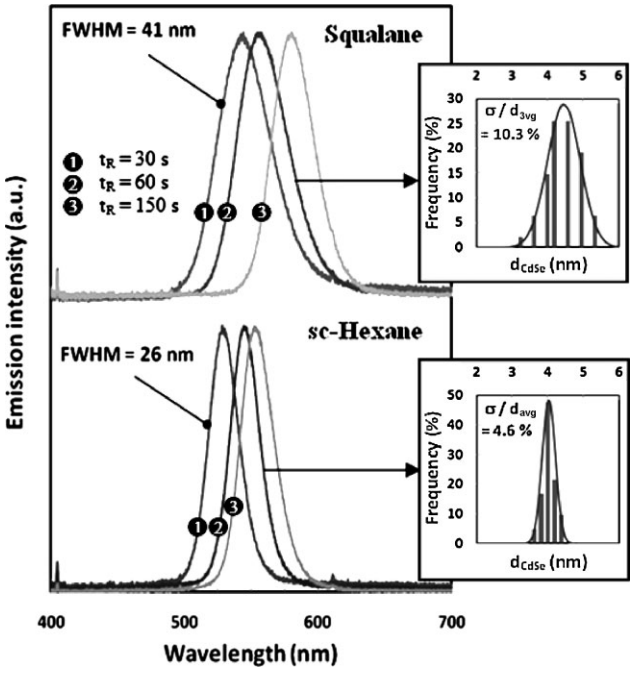

Figure 2. PL spectra at different residence times (t_R) obtained for CdSe QDs synthesized in Squalane and Hexane at 270 °C, 5 MPa with [Cd] = [Se] = 3.8×10^{-3} M and QD-size distributions obtained from TEM measurements for samples run at $R_t = 60$ s.

ADVANCED MATERIALS

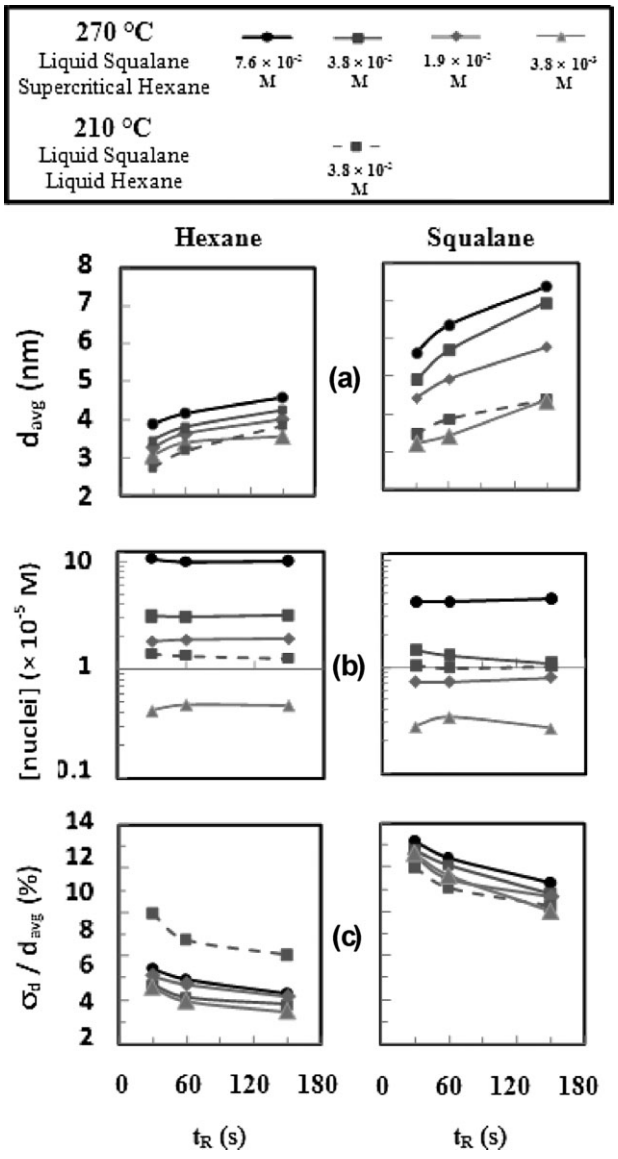

Figure 3. Results obtained for CdSe QDs synthesized in Squalane and Hexane as a function of the residence time (t_R) for different temperatures and concentrations of precursors: a) average diameter of QDs (nm), b) concentration of nuclei in the growth solution ($\times 10^{-5}$ M), and c) size distribution divided by the average QD diameter (%).

slight increase in the width of the size distribution with concentration can be explained by a broader residence-time distribution, as discussed below. This effect can be attributed to the lower diffusivity of the larger-sized nanoparticles in the solution.

Comparison between solvents shows that at a given residence time, QDs synthesized in sc-hexane are approximately 20 to 30% smaller than those synthesized in liquid squalane (Fig. 3a), while the concentration of the nuclei is 2 to 2.5 times higher in sc-hexane (Fig. 3b). The larger supersaturation in sc-hexane leads to a higher number of QDs. At equivalent reaction yields, this induces the synthesis of smaller-mean-size QDs.

A secondary factor that could contribute to decrease in size is the difference of dilatation between the squalane and the hexane. Such dilatation could lead to an increase in the fluid speed inside the channel when it reaches the high-temperature area, as well as a decrease of the speed when reaching the outlet of the microreactor. The average speed of the fluid in the microchannel is given by:

$$v = \frac{Q_v}{S} = \frac{Q_M M}{\rho S} \quad (1)$$

where Q_v is the volumetric flow rate, S is the cross-section surface of the channel, Q_M is the molar flow rate, M is the molar weight, and ρ is the fluid density. In our conditions, Q_M, M, and S are kept constant while ρ varies with temperature. Thus, we can estimate the speed of the solvent when reaching the high-temperature area, knowing the initial fluid speed:

$$\frac{v_{hot}}{v_{cold}} = \frac{\rho_{cold}}{\rho_{hot}} \quad (2)$$

where v_{hot} and ρ_{hot} are the speed of the fluid and its density in the hot area of the microreactor, while v_{cold} and ρ_{cold} are the same parameters in the cold area, respectively.

One can calculate that the speed of the sc-hexane will increase up to 1.8 times more than the speed of the squalane in the hot area. This effect could decrease the true residence time; however, by itself it cannot explain the smaller sizes observed for sc-hexane compared to squalane.

Notably, the use of supercritical fluid has a strong effect on the size distribution of the NCs, and consequently the full-width at half-maximum (FWHM) of the emission peak. Comparison of the data in Figure 3c shows that at 270 °C, for all precursor concentrations and residence times considered, the size distribution percentage (σ_d/d_{avg}) for QDs synthesized in sc-hexane, 4–6% (FWHM: 25–27 nm), is much smaller than for that for QDS synthesized in liquid squalane, 9–12% (FWHM: 41–49 nm). These results can be compared with the data from the literature for the highly optimized batch-mode synthesis of CdSe or CdS QDs in octadecene (ODE) or trioctylphosphine (TOP)/trioctylphosphine oxide mixtures ($\sigma_d/d_{avg} \approx 4$–7%, FWHM ≈25–30 nm).[26] For continuous experiments in high-temperature microreactors performed at 0.1MPa using high-boiling-point solvents, the size distributions range approximately from 7 to 11% for single-phase flow using squalane (FWHM = 30–39 nm),[9,13] and 6 to 8% for liquid–gas (squalane–argon) segmented flow (FWHM = 28–32 nm).[13] For liquid–liquid segmented flow using Fomblin Y 06/6 perfluorinated polyether as the carrier fluid and ODE as the reacting fluid, the reported size-distribution value is about 8% (FWHM = 34 nm).[14]

There are two main contributing factors to the variation in the size distribution: 1) Residence-time distribution (RTD) and 2) kinetics of nanocrystal formation. Single-phase fluid flow in microchannels is typically laminar, exhibiting a parabolic velocity profile. This means that during the growth

process QDs located near the channel walls will have a higher residence time compared to the QDs located near the center, where the velocity is faster. In general, a growing QD will undergo both axial dispersion and radial diffusion inside the fluid. Based on the size of the QD, the viscosity of the solvent, the fluid velocity, and the channel length, RTD curves can be calculated using Taylor dispersion model[27] for both squalane and hexane at 210 and 270 °C for $t_R = 30$ s (Fig. 4). Comparison of the curves shows that the width of the RTD is much narrower for hexane than for squalane, due to a 10- to 20-fold lower viscosity of hexane (Table 1). Note that temperature does not change the percentage in the residence-time distribution significantly.

Figure 3c shows that at 210 °C the observed size distribution in liquid hexane is 2% smaller than in squalane (dotted line) at the equivalent QD size. This is due primarily to the change in viscosity, leading to a variation in the RTD, as discussed above. Experiments run with hexane show that the main decrease of the size distribution is due to the supercritical phase of hexane at 270 °C, and not to the chemical structure of the solvents. It is also worth noting that the RTD effect is less pronounced at low flow rates, in particular for viscous flows. This can explain the slight narrowing of the size distribution with increasing residence times (Fig. 3c).

The final size distribution also depends on the kinetics of QD formation. As discussed above, the use of sc-hexane induces a higher initial concentration of nuclei for subsequent growth, compared to squalane (Fig. 3b). This results in the fast depletion of monomers in solution. Thus, the nucleation phase ends quickly, narrowing the initial size distribution. This behavior is only true at supercritical conditions for hexane. Indeed, synthesis in liquid hexane at 210 °C leads to the same concentration of nuclei as in liquid squalane. Therefore, we can assume that the nucleation rate is equivalent in the liquid phase, independent of the solvent used in this case.

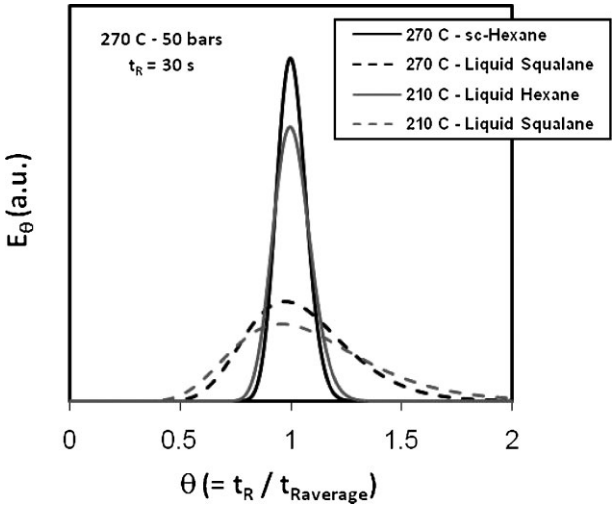

Figure 4. RTD curve calculated using a Taylor dispersion model for hexane and squalane at 210 °C, 5 MPa and 270 °C in a 400 μm ×250 μm ×1 m microchannel for a residence time of 30 s.

Based on the above considerations, several conclusions can be reached with this work. First, hexane (liquid or supercritical) results in a decrease of 2% in the size distribution of the QDs, due to the RTD effect caused by its lower viscosity compared to squalane. Most notably, the use of supercritical hexane leads to higher supersaturation compared to squalane, producing more nuclei and narrowing the size distribution further. We have demonstrated the synthesis of narrow emission CdSe QDs using a new continuous high-pressure process in supercritical hexane. Our work demonstrates the potentialities for materials synthesis in supercritical media in a continuous fashion at the microscale. The use of supercritical hexane is crucial in overcoming some of the limitations of high-boiling-point solvents (expensive, high viscosity, low diffusivity, and limited choice of precursors due to solubility consideration). More generally, the combination of microreactor synthesis with supercritical fluids provides for safer high-pressure processes as well as better reproducibility. The use of a high-pressure high-temperature microreactor, demonstrated in this work, opens new routes for nanomaterials synthesis in microfluidic devices, by enlarging the set of solvents (conventional low-boiling-point solvents) and phases (liquid, gas, supercritical) available.

Experimental

Microreactor Fabrication and Experimental Set-up: We have developed a Silicon-Pyrex microreactor working with modular compression fluidic connections (rubber O-rings). Other kinds of fluidic connections have been developed elsewhere [28], but require complicated microfabrication procedures to optimize the connection strength and are not versatile in terms of chemical compatibility. Compression sealing with rubber O-rings allows reaching theoretical pressure values up to 15 MPa or more [29]. The microreactor was fabricated using standard silicon-micromachining techniques. Channels were fashioned with deep reactive ion etching (DRIE) of silicon wafers ($\phi = 15$ cm, thickness = 0.8 mm). An oxide layer (0.5 μm) was grown on the surface, which was thereafter capped and sealed with anodically bonded pyrex wafers (thickness = 0.76 mm). High-pressure high-temperature fluidic connections were realized by compressing the microreactor between two aluminum parts using silicone O-rings (max operating temperature = 230 °C). Stainless steel tubings were connected to the compression part with conventional Swagelok fittings. The solutions (Cd and Se) were separately introduced in the microreactor using a high-pressure syringe pump (Harvard apparatus, PHD 22/2000 Hpsi). A heated aluminum block in contact with the reaction section of the device was used to control the temperature. The compression part is cooled down with a water flow to chill the quenching section. This set-up allows reaching high pressure (up to 15 MPa) and temperature (up to 350 °C in the heated section).

Preparation of Precursor Solutions: The solvents used for the CdSe QDs synthesis, hexane and squalane, were purchased from Aldrich and used as received. N_2 was purchased from Air Gas. Surfactants oleic acid, oleylamine, and TOP were purchased from Sigma–Aldrich. Cd precursor was prepared by reacting 1 mmol of $Cd(acac)_2$ and 1 mmol of oleic acid in octane at 125 °C under reflux (boiling point of octane is 125 °C). The solvent was removed after the complete dissolution of $Cd(acac)_2$ in the solution. The resulting product is redissolved in hexane, before the addition of oleylamine. In the case of squalane, we directly use the squalane as solvent. Se precursors were prepared by reacting Se shot and TOP at the concentration of 1.5 M, and then redissolving in hexane or squalane.

ADVANCED MATERIALS

Characterization Techniques: The absorbance and PL were determined using diluted solutions of the raw QD solution in hexane. Optical absorption spectra were acquired using a Hewlett Packard 8452 diode-array spectrometer. PL spectra were acquired using an Ocean optics SD2000 fiber-optic spectrometer and a handled UV lamp as an excitation source. TEM images of the QDs were obtained by depositing a drop of a diluted solution on a carbon-coated copper grid, prior to evaporation and analysis using a field-emission JEOL 2010 transmission electron microscope.

Received: June 9, 2008
Revised: August 12, 2008
Published online: October 22, 2008

[1] a) M. Bruschez, Jr, M. Moronne, P. Gin, S. Weiss, A. P. Alivisatos, *Science* **1998**, *281*, 2013. b) W. Liu, M. Howarth, A. B. Greytak, Y. Zheng, D. G. Nocera, A. Y. Ting, M. G. Bawendi, *J. Am. Chem. Soc.* **2008**, *130*, 1274.
[2] S. Coe, W. K. Woo, M. G. Bawendi, V. Bulovic, *Nature* **2002**, *420*, 800.
[3] a) V. I. Klimov, A. A. Mikhailovsky, S. Xu, A. Malko, J. A. Hollingsworth, C. A. Leatherdale, H. J. Eisler, M. G. Bawendi, *Science* **2000**, *290*, 314. b) M. Kazes, D. Y. Lewis, Y. Ebenstein, T. Mokari, U. Banin, *Adv. Mater.* **2002**, *14*, 317.
[4] K. F. Jensen, *Chem. Eng. Sci.* **2001**, *56*, 293.
[5] a) K. F. Jensen, *Silicon MRS Bull.* **2006**, *31*, 101. b) T. Gervais, K. F. Jensen, *Chem. Eng. Sci.* **2006**, *61*, 1102.
[6] H. Nakamura, Y. Yamaguchi, M. Miyasaki, M. Uehara, H. Maeda, P. Mulvaney, *Chem. Commun.* **2002**, 2844.
[7] N. de Mas, A. Guenther, T. Kraus, M. A. Schmidt, K. F. Jensen, *Ind. Eng. Chem. Res.* **2005**, *44*, 8997.
[8] T. M. Squires, S. R. Quake, *Rev. Mod. Phys.* **2005**, *77*, 977.
[9] B. K. H. Yen, N. E. Stott, K. F. Jensen, M. G. Bawendi, *Adv. Mater.* **2003**, *15*, 1858.
[10] H. Song, J. D. Tice, R. F. Ismagilov, *Angew. Chem. Int. Ed.* **2003**, *42*, 768.
[11] A. Günther, S. Khan, M. Thalmann, F. Trachsel, K. F. Jensen, *Lab Chip* **2004**, *4*, 278.
[12] A. Günther, M. Jhunjhunwala, M. Thalmann, M. A. Schmidt, K. F. Jensen, *Langmuir* **2005**, *21*, 1547.
[13] B. K. H. Yen, A. Gunther, M. A. Schmidt, K. F. Jensen, M. G. Bawendi, *Angew. Chem. Int. Ed.* **2005**, *44*, 5447.
[14] E. M. Chan, A. P. Alivisatos, R. A. Mathies, *J. Am. Chem. Soc.* **2005**, *127*, 13854.
[15] C. Eckert, B. L. Knutson, P. G. Debenedetti, *Nature* **1996**, *383*, 313.
[16] a) E. Reverchon, R. Adami, *J. Supercrit. Fluids* **2006**, *37*, 1. b) S. Marre, F. Cansell, C. Aymonier, *Langmuir* **2008**, *24*, 252.
[17] a) C. Aymonier, A. Erriguible, S. Marre, A. Serani, F. Cansell, *Processes Int. J. Chem. React. Eng.* **2007**, *5*, A77. b) C. Aymonier, A. Loppinet-Serani, H. Reveron, Y. Garrabos, F. Cansell, *J. Supercrit. Fluids* **2006**, *38*, 242.
[18] F. Benito-Lopez, R. M. Tiggelaar, K. Salbut, J. Huskens, R. J. M. Egberink, D. N. Reinhoudt, H. J. G. E. Gardeniers, W. Werboom, *Lab Chip* **2007**, *7*, 1345.
[19] J. Kobayashi, Y. Mori, S. Kobayashi, *Chem. Commun.* **2005**, *20*, 2567.
[20] a) J. D. Holmes, K. J. Ziegler, R. C. Doty, L. E. Pell, K. P. Johnston, B. A. Korgel, *J. Am. Chem. Soc.* **2001**, *123*, 3743. b) X. Lu, K. J. Ziegler, A. Ghezelbach, K. P. Johnston, B. A. Korgel, *Nano Lett.* **2004**, *4*, 969.
[21] F. Trachsel, C. Hutter, P. Rudolf von Rohr, *Chem. Eng. J.* **2008**, *135S*, S309.
[22] These values were obtained from the NIST online chemistry webbook, see: http://webbook.nist.gov/chemistry/fluid/.
[23] Physical properties of Squalane (density, viscosity) as a function of pressure and temperature were extrapolated from experimental values and model from O. Fandino, A. S. Pensado, M. J. P. Comunas, J. Fernandez, *J. Chem. Eng. Data* **2005**, *50*, 939 and U. G. Krahn, G. Luft, *J. Chem. Eng. Data* **1994**, *39*, 670.
[24] C. B. Murray, D. J. Norris, M. G. Bawendi, *J. Am. Chem. Soc.* **1993**, *115*, 8706.
[25] C. A. Leatherdale, W. K. Woo, F. V. Mikulec, M. G. Bawendi, *J. Phys. Chem. B* **2002**, *106*, 7619.
[26] a) Q. Dai, D. Li, S. Jiang, H. Chen, Y. Wang, S. Kan, B. Liu, Q. Cui, G. Zou, *J. Cryst. Growth* **2006**, *292*, 14. b) W. W. Yu, X. Peng, *Angew. Chem. Int. Ed.* **2002**, *41*, 2368. c) Z. A. Peng, X. Peng, *J. Am. Chem. Soc.* **2001**, *123*, 183.
[27] a) O. Levenspiel, in *Chemical Reaction Engineering*, 3rd Ed., Wiley, New York, U.S.A **1999**. b)O. Levenspiel, W. K. Smith, *Chem. Eng. Sci.* **1957**, *6*, 227. Calculations of the diffusivity for both solvents were obtained from the Stokes-Einstein equation $D = kT/6\pi\eta a$, using a particles size $a = 1$ nm. Note that the value of a strongly influences the value of D.
[28] a) A. V. Pattekar, M. V. Kothare, *J. Micromech. Microeng.* **2003**, *13*, 337. b) M. Tiggelaar, F. Benito-Lopez, D. C. Hermes, H. Rathgen, R. J. M. Egberink, F. G. Mugele, D. N. Reinhoudt, A. van den Berg, W. Werboom, H. J. G. E. Gardeniers, *Chem. Eng. J.* **2007**, *131*, 163. c) Y. Peles, V. T. Srikar, T. S. Harrison, C. Protz, A. Mracek, S. M. Spearing, *J. Microelectromech. Syst.* **2004**, *13*, 31. d) M. T. Blom, E. Chmela, J. G. E. Gardeniers, J. W. Berenschot, M. Elwenspoek, R. Tijssen, A. van den Berg, *J. Micromech. Microeng.* **2001**, *11*, 382.
[29] L. Szekely, R. Freitag, *Anal. Chim. Acta* **2004**, *512*, 39.